Chapter 4

Scientific Results and Interpretation

4.1 Interferometric Phase Shifting Technique combined with off-axis illumination

The thick and tilted beam splitter between the projection lens and the wafer causes serious optical aberrations in the original interferometric phase shifting arrangement. To address this issue, the IPS technique was combined with off-axis illumination ($IPS - OAI$ method). However, two-beam imaging – one of the most serious limitations of off-axis illumination – could significantly degrade the final image contrast. In this section, it will be shown theoretically and experimentally that the $IPS - OAI$ combination technique could address both limitations mentioned above for line/space patterns [63, 64, 65, 66, 67].

4.1.1 Theoretical Results

The mask illumination is a key process in the $IPS - OAI$ method in which a Mach-Zehnder interferometer is used to illuminate the mask almost symmetrically from front and back sides simultaneously. The system is optimized so that only four diffraction orders – the transmitted and the reflected zero and first orders – contribute to the final image ("four-beam imaging"). The imaging process can be considered as a coherent superposition of two images. The first (R) image is generated by the reflected zero and first orders, and the second (T) image is generated by the transmitted zero and first orders. First of all let us describe the interaction between these two images. Fig. (4.1) depicts a schematic view of the principle of four beam imaging. The off-axis angle is optimized so that the diffraction angle (β) be closely equal to the off-axis angle (α). The transmitted zero ($E_0^t(x,z,t)$) and first ($E_1^t(x,z,t)$), and the reflected zero ($E_0^r(x,z,t)$) and first ($E_1^r(x,z,t)$) diffraction orders can be written as:

$$E_0^t(x,z,t) = \hat{E}_0^t \cdot sin\left(\omega t - \frac{2\pi}{\lambda} sin(\alpha) \cdot x - \frac{2\pi}{\lambda} cos(\alpha) \cdot z\right) \tag{4.1a}$$

$$E_1^t(x,z,t) = \hat{E}_1^t \cdot sin\left(\omega t + \frac{2\pi}{\lambda} sin(\alpha) \cdot x - \frac{2\pi}{\lambda} cos(\alpha) \cdot z\right) \tag{4.1b}$$

$$E_0^r(x,z,t) = \hat{E}_0^r \cdot sin\left(\omega t - \frac{2\pi}{\lambda} sin(\alpha) \cdot (x-\Delta) - \frac{2\pi}{\lambda} cos(\alpha) \cdot z + \Psi\right) \tag{4.1c}$$

$$E_1^r(x,z,t) = \hat{E}_1^r \cdot sin\left(\omega t + \frac{2\pi}{\lambda} sin(\alpha) \cdot (x-\Delta) - \frac{2\pi}{\lambda} cos(\alpha) \cdot z + \Psi\right), \tag{4.1d}$$

where, Δ $(= \frac{\lambda}{4 \cdot sin\alpha})$ is the spatial shift between R and T images, Ψ is an arbitrary phase difference between the reflected and the transmitted beams, and (x, z) are spatial coordinates defined in Fig. (4.1). In an ideal case, when the reflection of the chrome layer and the transmission of the substrate are unity, the amplitudes can be given as follows:

$$\frac{\hat{E}_1^t}{\hat{E}_0^t} = \frac{\hat{E}_1^r}{\hat{E}_0^r} = \frac{2}{\pi} \tag{4.2a}$$

$$\frac{\hat{E}_0^t}{\hat{E}_0^r} = t, \tag{4.2b}$$

where t is the amplitude ratio of beams that illuminate the mask from the back and front sides. However, if we take into consideration that the reflectivity of the chrome layer R_{Cr} is not 1 but 0.71 and the Fresnel reflection at the transmitting surfaces of the mask is not 0 but R_{Sub}=0.032, then the amplitude ratio of the reflected first and zero diffraction orders is modified as follows:

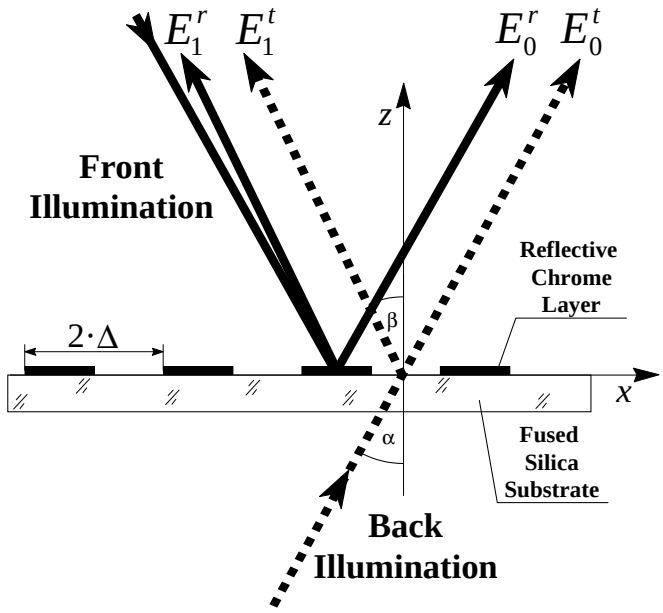

Figure 4.1: Four-beam imaging

$$\frac{\hat{E}_1^r}{\hat{E}_0^r} = \frac{2}{\pi} \cdot \frac{\sqrt{R_{Cr}} - \sqrt{R_{Sub}}}{\sqrt{R_{Cr}} + \sqrt{R_{Sub}}} \approx 0.41, \tag{4.3}$$

and the contrast reduces to about 70.5% from the original 90.6% value (Eq. 2.7). The total intensity distribution is represented by the time average value of the square of the sum of the electric fields (Eq. 4.1a-d):

$$I(x,z) = \frac{1}{2\pi}\int_0^{2\pi} \left[E_0^t(x,z,t) + E_1^t(x,z,t) + E_0^r(x,z,t) + E_1^r(x,z,t)\right]^2 d(\omega t). \qquad (4.4)$$

The intensity distributions using different amplitude and phase conditions can be seen in Fig. (4.2). The first column shows the calculated results. In case *a* only the reflected zero and first diffraction orders, while in case *b* the transmitted diffraction orders contribute to the image. The two images are spatially shifted by half the period of the line/space pattern (Δ). It means that where the R image has minima, T image has maxima. The contrast of both R and T images is 70.5%. This limitation of off-axis illumination called "two-beam imaging" was discussed in Section 2.1.2. However, using the four-beam imaging approach instead of two-beam imaging, the initial phase and amplitude conditions could be optimized so that the contrast of the final image could reach the maximum 100% value. The conditions that must be satisfied are the following:

Condition 1 *The peak intensity of the transmitted pattern must be equal to the minimum intensity of the reflected pattern.*

Condition 2 *The phase difference between R and T images must be π, i.e. the images must be in the opposite phase.*

If these optimized illumination conditions are satisfied, then the contrast of the final image (Fig. 4.2.c) could reach the maximum 100% value. When the phase shift between the transmitted and the reflected images is set to 0 (or $k \cdot 2\pi$, where k is an integer), the contrast could reduce to 30% (Fig. 4.2.d). These calculations show that the system is extremely phase sensitive. A $\lambda/4$ mirror translation ($\approx 0.11\mu m$ @ $457.8nm$) means that the system shifts from the optimum to the worst setup. Therefore, during the experiment special attention was paid to eliminate every undesirable vibration effect.

4.1.2 Experimental Results

The experimental arrangement can be seen in Fig. (4.3). The output from a continuous wave Ar^+-ion laser operating at 457.9 nm was split into two beams and used to illuminate the mask. The mask was a patterned evaporated, reflective chrome layer on a fused silica substrate, forming a line/space pattern, with a spatial frequency of 16 μm. The intensity and the phase of the back illumination was controlled by a variable attenuator and a piezo-controlled linear translator, respectively. A microscope objective (L_1: magnification $M_1 = 20X, NA_1 = 0.4$) produced the image. The mask to objective distance

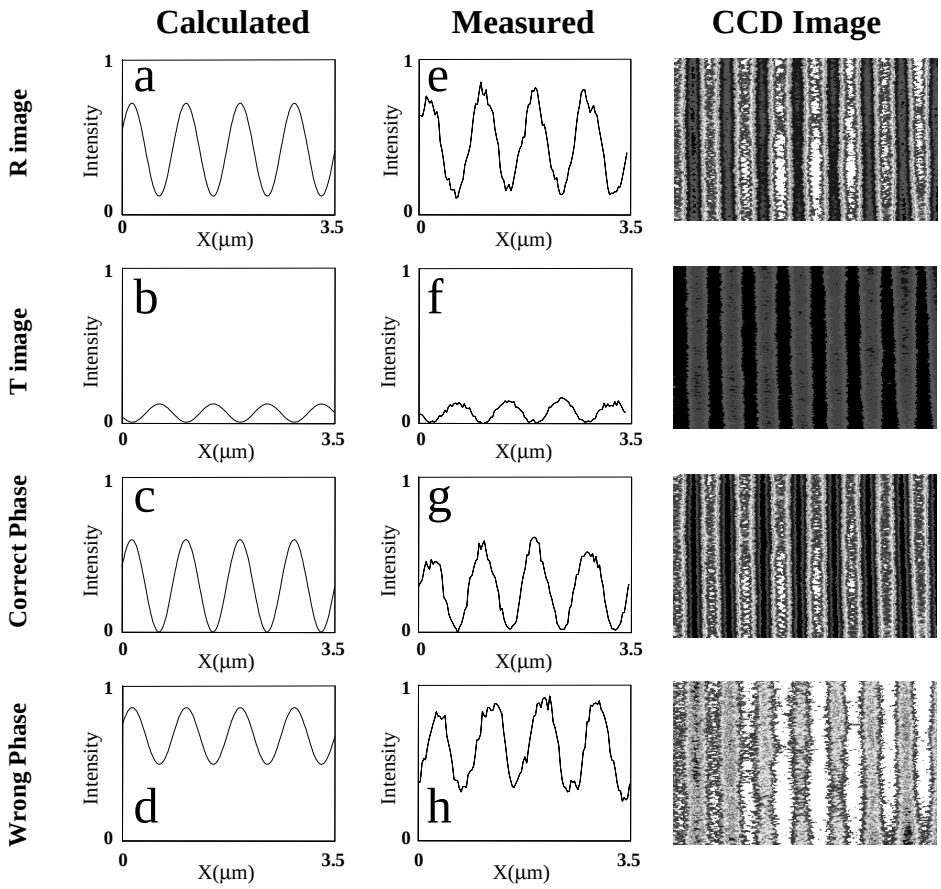

Figure 4.2: Intensity pattern as observed by the CCD camera.

was adjusted to the manufacturer microscope tube length to ensure a nominal magnification ratio and high image quality. The off-axis illumination angle of the mask was 1° and the first order diffraction angle was 0.7°. Thus, the microscope objective, which had a numerical aperture of $0.4/20 = 0.02$ on the mask side, would accept only the 0 and $+1$ order beams propagating at a relative angle of 1.7° while all other diffraction orders were rejected. The image of the line/space pattern formed by lens L_1 was magnified by means of two microscope objectives L_2 and L_3 in tandem ($M_2 = 20X, NA_2 = 0.5$ and $M_3 = 40X, NA_3 = 0.65$). The imaging lens L_2 was mounted on a precision translator allowing a direct measurement of the depth of focus of the image. The magnified image was projected onto a CCD camera by lenses L_2 and L_3, which were only used for image diagnostics. The second column in Fig. (4.2) depicts the experimental results recorded by a CCD camera. The measured value of contrast of the R image is 68.7% as shown in Fig. (4.2.e). This value agrees very closely with the calculated 70.5% value. In case f (T image) the beam amplitude coming from the back arm of the interferometer was attenuated so that **Condition 2** could be satisfied. In case g when both the reflected

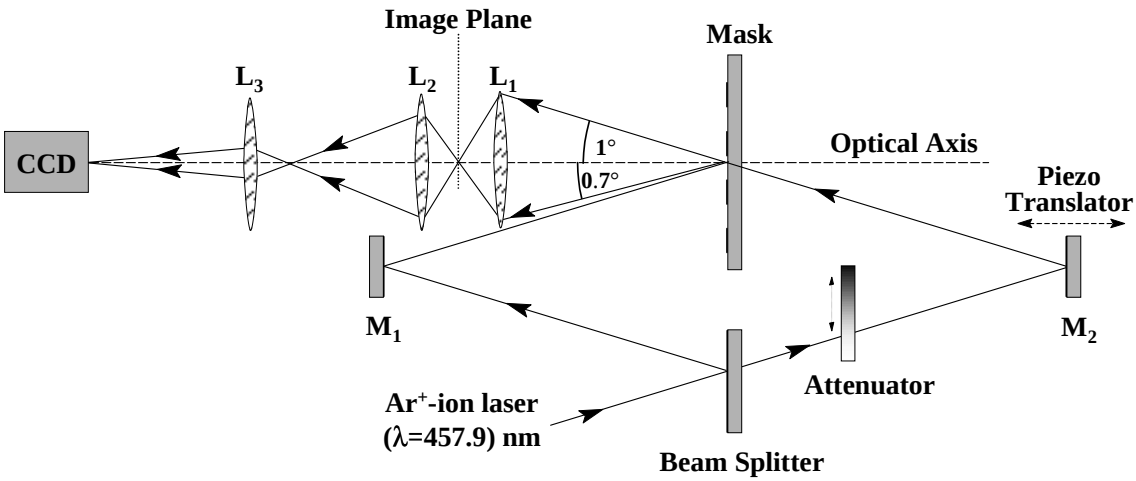

Figure 4.3: Experimental scheme for off-axis illumination combined with interferometric phase shifting.

and the transmitted diffraction orders play part in the imaging process under optimum conditions (both amplitude and phase conditions are satisfied), the contrast of the image is nearly 100%, i.e. the intensity minima between the main peaks are almost 0. When the phase difference between T and R images is 0 (case h), the contrast significantly decreases. The third column in Fig. (4.2) shows the images as were captured by the CCD camera as a reference.

The image of the line/space pattern was also recorded in an experimental Shipley XP 94314 photoresist. An about 0.5 μm thick photoresist layer was deposited on a 1 inch diameter silica wafer. During photoresist exposure, the resist was placed directly in the image plane of lens L_1. A beam with an energy density of 40 mJ/cm^2 was used to expose the resist. The develpement time was 60 seconds with Shipley MF 320 developer. An atomic force microscope (Park Scientific Instruments) image of the exposed photoresist is shown in Fig. (4.4). A significant fraction of the sidewall slope seen here is due to the limited resolv-

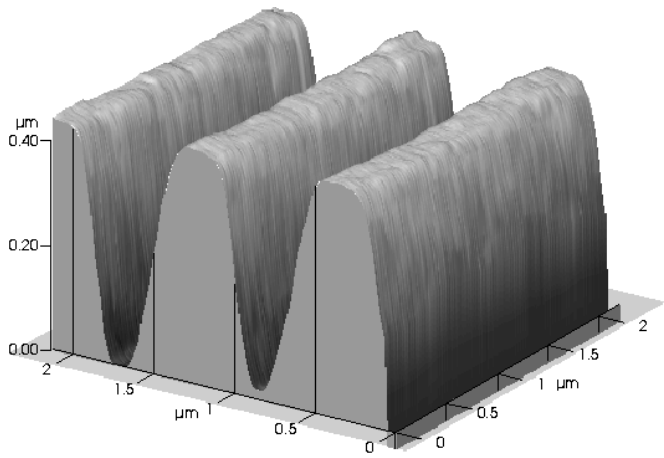

Figure 4.4: AFM photograph of the line/space pattern produced on photoresist.

ing power of the AFM microscope tip. However, an upper limit can be given for the minimum feature size of the exposed line/space pattern that can be compared with the preliminary calculated value of CD. The calculated 0.4 μm value agrees with the period of the exposed pattern. Since the theoretical resolution limit of a traditional imaging system with $NA = 0.4$ at $\lambda = 457.9$ nm for line/space patterns ($k_1 = 1/2$) is 0.57 μm (Eq. 2.1), we can say that the $IPS - OAI$ technique can improve the resolution by 30% for line/space patterns. In addition to this significant resolution enhancement, due to the high spatial coherence of the illuminating laser beam, a high image contrast results in approximately 5 μm defocus in both directions.

Since the method does not require a phase shifting layer on the mask, it eliminates all issues related to phase shifting mask manufacturing and cleaning. The technique can be implemented into 248 and 193 nm stepper systems, however, innovative stepper design may be necessary.

The proposed combination technique, however, requires optical elements with flatness smaller than $\lambda/72$ @ 248nm. Due to these issues, the $IPS - OAI$ combination technique can mainly be used as an effective and inexpensive test-bed for studying various phase shifting schemes combined with off-axis illumination, rather than a direct process installed into a stepper system.

Because of the ability to adjust the relative phase and amplitude of the two (front and back) illuminating beams, this method is capable of the evaluation of several kinds of $PS - OAI$ combination techniques. The phase shifting masks can be substituted with a simple chrome mask using the following correspondences:

Conventional Phase Shifting Techniques		**Interferometric Approach**
$Transparent\ part$	$\Longrightarrow$	$Transparent\ part$
$Phase\ shifting\ part$	$\Longrightarrow$	$Chrome\ part$
$Chrome\ part$	$\Longrightarrow$	$Dark\ field\ grating\ part\ (with\ chrome)$
$Dark\ field\ grating\ (with\ PS\ layer)$	$\Longrightarrow$	$Dark\ field\ grating\ (with\ chrome)$